Cooperative distributed LQR control for longitudinal flight of a formation of non-identical low-speed experimental UAV's

Eleftherios E. Vlahakis
School of Mathematics, Computer Science and Engineering,
City, University of London, UK
eleftherios.vlahakis@city.ac.uk

Efstathios Milonidis
School of Mathematics, Computer Science and Engineering,
City, University of London, UK
e.milonidis@city.ac.uk

George D. Halikias
School of Mathematics, Computer Science and Engineering,
City, University of London, UK
g.halikias@city.ac.uk

***Abstract*—In this paper, an established distributed LQR control methodology applied to identical linear systems is extended to control arbitrary formations of non-identical UAV's. The non-linear model of a low-speed experimental UAV known as X-RAE1 is utilized for simulation purposes. The formation is composed of four dynamically decoupled X-RAE1 which differ in their masses and their products of inertia about the xz plane. In order to design linear controllers the nonlinear models are linearized for horizontal flight conditions at constant velocity. State-feedback, input and similarity transformations are applied to solve model-matching type problems and compensate for the mismatch in the linearized models due to mass and symmetry discrepancies among the X-RAE1 models. It is shown that the method is based on the controllability indices of the linearized models. Distributed LQR control employed in networks of identical linear systems is appropriately adjusted and applied to the formation of the non-identical UAV's. The applicability of the approach is illustrated via numerous simulation results.**

***Keywords*—Cooperative distributed LQR, formation control, non-identical agents, UAV, model-matching.**

I. Introduction

Multi-vehicle systems have attracted a lot of attention of the control community in recent years due to their wide range of applications, such as area mapping and monitoring [1], formation control [2], [3], vehicle platoons [4], etc. Such schemes are often referred to as multi-agent systems with each agent being represented by a dynamical system and having the ability to communicate with other counterparts within the network. The interactions established among the agents determine the network topology and define a communication pattern. The need for forming networks of systems in many cases arises from the fact that some problems might not be resolved by individual systems.

Stability issues play key role in multi-vehicle systems [2], [5] where cooperative controllers should be designed to ensure stable operation for the network. Two complementary distributed LQR methods are proposed in [6] and [7]. In the first (top-down) approach [6], the centralized optimal LQR controller is approximated by a distributed control scheme whose stability is guaranteed by the stability margins of LQR control. The second [7] consists of a bottom-up approach in which optimal interactions between self-stabilizing agents are defined so as to minimize an upper bound of the global LQR criterion. A limitation of both methods is the assumption that networks are formed by identical plants, a fact which is often unrealistic in real applications. For background theory and fundamental results in the area of cooperative control over networks see [8].

In [3] the distributed LQR method introduced in [6] is used to solve the formation control problem of a network of identical UAV's. In this work, we extend this top-down approach to networks formed of non-identical UAV's. The non-linear model of the low-speed experimental UAV used in [3] known as X-RAE1 is also utilized in this paper for simulations purposes. The formation flying is considered to be composed of dynamically decoupled X-RAE1 which differ in their masses and their symmetry about the xz plane. In order to design linear controllers the nonlinear models are linearized for horizontal flight conditions at constant velocity. State-feedback, input and similarity transformations are applied to solve model-matching type problems and compensate for the mismatch in the linearized models due to mass and symmetry discrepancies among the X-RAE1 models. To our knowledge no direct extension method of distributed LQR control with non-identical dynamics based on the methodology of [6] and [7] has been reported in the literature. The distributed LQR method proposed in [3] to solve the formation control of four identical UAV's is appropriately adjusted and applied to the formation of the non-identical UAV's. Note that, in contrast to recent methods in the area, our approach does not rely on a two-step design procedure in which high-level formation control based exclusively on kinematics is superimposed on a low-level flight control scheme of each individual UAV in the formation, based on a fully dynamic model. We show the applicability of our approach via numerous simulation results.

The rest of the paper is organized in five sections. First, in Section II preliminaries on graph theory and Kronecker products are presented. In Section III the nonlinear and the linearized models for certain operating point of four X-RAE1's are introduced. In Section IV model-matching approach is proposed to compensate for discrepancies among the linearized

models of four non-identical UAV's of a formation flying followed by a distributed LQR methodology to solve the formation control problem. In Section V simulation results are presented while the conclusions of the paper appear in Section VI.

II. Preliminaries

A graph $\mathscr{G}$ is defined as $\mathscr{G} = (\mathscr{V}, \mathscr{E})$, where $\mathscr{V}$ is the set of nodes (or vertices) $\mathscr{V} = \{1, \cdots, N\}$ and $\mathscr{E} \subseteq \mathscr{V} \times \mathscr{V}$ the set of edges (i, j) with $i \in \mathscr{V}$, $j \in \mathscr{V}$. The degree d_j of a graph vertex j is the number of edges which start from j. Let $d_{max}(\mathscr{G})$ denote the maximum vertex degree of the graph $\mathscr{G}$. We denote by $\mathbf{A}(\mathscr{G})$ the (0, 1) adjacency matrix of the graph $\mathscr{G}$. Let $\mathbf{A}_{i,j} \in \mathbb{R}$ be its i, j element, then $\mathbf{A}_{i,j} = 1$ if $(i, j) \in \mathscr{E}$, $\forall i, j = 1, \cdots, N$, $i \neq j$. Let $j \in \mathscr{N}_i$ represent the neighbourhood of the i^{th} node if $(i, j) \in \mathscr{E}$ and $i \neq j$. The adjacency matrix $\mathbf{A}(\mathscr{G})$ of undirected graphs is symmetric. We define the Laplacian matrix as $L(\mathscr{G}) = \mathbf{D}(\mathscr{G}) - \mathbf{A}(\mathscr{G})$ where $\mathbf{D}(\mathscr{G})$ is the diagonal matrix of vertex degrees d_i (also called the valence matrix).Let $S(\mathbf{L}(\mathscr{G})) = \{\lambda_1(\mathbf{L}(\mathscr{G})), \cdots, \lambda_N(\mathbf{L}(\mathscr{G}))\}$ be the spectrum of the Laplacian matrix $\mathbf{L}$ associated with an undirected graph $\mathscr{G}$ arranged in nondecreasing semi-order. Further definitions and results on graph theory can be found in [9]. The Kronecker product of $A = [a_{ij}] \in \mathbb{R}^{m \times n}$ and $B = [b_{ij}] \in \mathbb{R}^{p \times q}$ is denoted by $A \otimes B \in \mathbb{R}^{mp \times nq}$.

III. Modelling of XRAE1

A. Equations of motion

The aircraft's model has been obtained from [3], [10]. The equations of the longitudinal and the lateral motions are considered. Six equations of motion describe the dynamical behavior of the X-RAE1 with respect to longitudinal and lateral modes of the aircraft. Three more equations give the relationship between the Euler-angle rates and the body-axis rates. The corresponding nonlinear differential equations are given next.

1) Three Translational equations of motion along the x, y and z body axes:

$$\begin{aligned}
\dot{U} &= RV - QW - g\sin\Theta \\
&\quad + [qS(C_L \sin a - C_D \cos a) + T]/m \\
\dot{V} &= PW - RU + g\cos\Theta\sin\Phi) + (qSC_y)/m \\
\dot{W} &= QU - PV + g\cos\Theta\cos\Phi \\
&\quad + [qS(-C_L \cos a - C_D \sin a)]/m
\end{aligned}$$

2) Three Rotational equations of motion around the x, y and z body axes:

$$\begin{aligned}
\dot{P}I_x - \dot{R}I_{xz} &= QR(I_y - I_z) + PQI_{xz} + qSbC_l \\
\dot{Q}I_y &= PR(I_z - I_x) - (P^2 - R^2)Ixz + qScC_m \\
&\quad + qS(C_L \sin a - C_D \cos a)h_0 + Te_T \\
\dot{R}I_z - \dot{P}I_{xz} &= PQ(I_x - I_y) + QRI_{xz} + qScC_n
\end{aligned}$$

3) Relationship Between Euler-Angle Rates and Body-Axis Rates:

$$\begin{bmatrix} \dot{\Phi} \\ \dot{\Theta} \\ \dot{\Psi} \end{bmatrix} = \begin{bmatrix} 1 & \sin\Phi\tan\Theta & \cos\Phi\tan\Theta \\ 0 & \cos\Phi & -\sin\Phi \\ 0 & \sin\Phi\sec\Theta & \cos\Phi\sec\Theta \end{bmatrix} \begin{bmatrix} P \\ Q \\ R \end{bmatrix}$$

where

- U, V, W represent forward, side and downward velocities along the x, y and z body axes, respectively.
- P, Q, R represent roll, pitch and yaw angular velocities around the x, y and z body axes, respectively.
- Φ, Θ, Ψ represent roll, pitch and yaw angles.
- T is the thrust.
- C_L, C_D, C_y are lift, drag and side force coefficients.
- I_x, I_y and I_z are moments of inertia about the corresponding body axes.
- I_{xz} is the product of inertia. $I_{xy} = I_{yz} = 0$ since xz is a plane of symmetry of the aircraft.
- a, q are the angle of attack and the dynamic pressure, respectively.
- m, g, S, e_T, h_0, b and c are known parameters.

Detailed description of the above variables and values of the corresponding parameters can be found in [10].

B. Linearization about operating point

For a straight, steady, symmetric and horizontal flight the nonlinear model of the aircraft's motion can be replaced by the linearized version provided the perturbations about the nominal operating conditions are sufficiently small. Thus the control design may be carried out on the linear model and linear controllers can be constructed. The linearized equations of motion are separated into longitudinal and lateral-directional equation sets. Since the two inputs (thrust and elevator) employed in longitudinal motion do not affect the lateral motion due to symmetry of the xz aircraft's plane, the two linearized models (longitudinal and lateral) are dynamically decoupled in the case of height control. In this work we are interested in the longitudinal stability of networks of non-identical X-RAE1's about operating points which are called trim conditions. For simulation purposes, different mass m_i and product of inertia I_{xz_i} for each system have been considered. This mismatch which in real applications might arise for non-identical payloads, leads to different linearized models for each X-RAE1. At a constant velocity $V_{T_0} = 30ms^{-1}$ the trim conditions for the i^{th} X-RAE1's is:

$$\begin{aligned}
&U_{0i} = V_{T_0}\cos a_{0i}, \quad W_{0i} = V_{T_0}\sin a_{0i}, \quad \Theta_{0i} = a_{0i} \\
&V_{0i} = P_{0i} = Q_{0i} = R_{0i} = 0, \quad \Phi_{0i} = \Psi_{0i} = 0
\end{aligned} \tag{1}$$

The state-space form of the linearized model for the longitudinal motion of the i^{th} aircraft takes the form

$$\dot{x}_i = A_i x_i + B_i u_i, \quad x_i(0) = x_{i0} \tag{2}$$

where $x_i = \begin{bmatrix} u_i & w_i & q_i & \theta_i & h_i \end{bmatrix}^T$ and $u_i = \begin{bmatrix} n_i & \delta_{T_i} \end{bmatrix}^T$ represent the deviation of the state and input vector, respectively, from the trimmed values (i.e., $U_i - U_{0i} = u_i$). Note that in our linear model (2) an additional variable has been included which represents height deviation h_i from a desired reference point. This augmentation can be used to provide asymptotic tracking of step references. Table I shows the selection of mass and product of inertia of four X-RAE1 models and Table II illustrates the mismatch in the corresponding A_i and B_i matrices.

TABLE I
MASS AND PRODUCT OF INERTIA OF FOUR X-RAE1 MODELS

X-RAE1	m_i $[kg]$	I_{xz} $[kg \cdot m^2]$
agent-1	18.5	0.17
agent-2	20.5	0.26
agent-3	16.5	0.08
agent-4	15.5	0.26

TABLE II
DYNAMICS AND INPUT MATRICES (A,B) OF FOUR LINEAR MODELS.

X-RAE1	A_i					B_i	
agent-1	−0.142	−0.227	2.493	−9.771	0	−1.136	1.444
	−1.033	−4.476	28.639	0.837	0	−13.060	0
	−0.042	−2.744	15.351	−0.134	0	−137.157	−2.036
	0	0	1	0	0	0	0
	−0.087	−0.996	0	30	0	0	0
agent-2	−0.125	−0.155	2.264	−9.773	0	−0.928	1.3032
	−0.963	−4.053	28.780	0.758	0	−11.811	0
	−0.022	−2.836	15.383	−0.122	0	−137.399	−2.036
	0	0	1	0	0	0	0
	−0.078	−0.997	0	30	0	0	0
agent-3	−0.163	−0.317	2.717	−9.764	0	−1.392	1.619
	−1.120	−5.002	28.468	0.915	0	−14.605	0
	−0.059	−2.636	15.315	−0.147	0	−136.867	−2.036
	0	0	1	0	0	0	0
	−0.095	−0.995	0	30	0	0	0
agent-4	−0.175	−0.370	2.826	−9.760	0	−1.545	1.724
	−1.171	−5.314	28.367	0.954	0	−15.525	0
	−0.065	−2.573	15.294	−0.153	0	−136.670	−2.036
	0	0	1	0	0	0	0
	−0.099	−0.995	0	30	0	0	0

IV. DISTRIBUTED CONTROL FOR NON-IDENTICAL UAV'S

As Table II illustrates, the four linearized models obtained for operating conditions specified earlier are not identical due to discrepancies in mass and product of inertia among the X-RAE1's. This drawback renders the distributed LQR method presented in [6] and utilized in [3] not directly applicable to enforce longitudinal stability of a formation of X-RAE1's. In this section, first a model-matching approach to overcome the mismatch among non-identical linear systems is presented for a certain class of linear systems and then the cooperative distributed control method utilized in [3] is extended to the case of non-identical UAV's.

A. Model-Matching of multi-input systems with common controllability indices

The aim of the method shown in this paragraph is to map a set of linear systems to a common target system specified a priori via state-feedback, similarity and input transformations. The class of systems to be considered consists of multi-input systems with fixed controllability indices μ_j. Recall that $\sum_{j=1}^{m} \mu_j = n$ where m stands for the number of inputs and n the state dimension. Note that the controllability indices define completely the class without the need for specifying input and state sizes. The following Lemma is standard and is included without proof (see [11] for details).

Lemma 1. *Given (A,B) controllable, then $(P(A+BF)P^{-1}$, $PBG)$ has the same controllability indices, up to reordering, for any P, F and G ($det(P) \neq 0$, $det(G) \neq 0$) of appropriate dimensions.*

The controller canonical form of a multi-input plant is now analyzed. Let the pair (A, B) be controllable with controllability indices $\{\mu_j\}$ where $A \in \mathbb{R}^{n\times n}$ and $B \in \mathbb{R}^{n\times m}$. There is always similarity transformation P (see [11] for how to construct matrix P) such that the pair can be reduced to controller canonical form, namely, (A_c, B_c) where

$$A_c = \bar{A}_c + \bar{B}_c A_m, \quad B_c = \bar{B}_c B_m \tag{3}$$

with $A_m \in \mathbb{R}^{m\times n}$ and $B_m \in \mathbb{R}^{m\times m}$ being free. The pair ($\bar{A}_c$, $\bar{B}_c$) is called the Brunovsky canonical form [11] and is unique (up to reordering) for the class of pairs (A_i, B_i) with common controllability indices. The matrices $(\bar{A}_c, \bar{B}_c) = (\text{diag}(\bar{A}_{11}, \cdots, \bar{A}_{mm}), \text{diag}(\bar{B}_{11}, \cdots, \bar{B}_{mm}))$ where

$$\bar{A}_{jj} = \begin{bmatrix} 0 & \\ \vdots & I_{\mu_j - 1} \\ 0 & \\ 0 & 0 \cdots 0 \end{bmatrix} \in \mathbb{R}^{\mu_j \times \mu_j}, \; \bar{B}_{jj} = \begin{bmatrix} 0 \\ \vdots \\ 0 \\ 1 \end{bmatrix} \in \mathbb{R}^{\mu_j} \text{ for } j = 1, \cdots, m.$$

Theorem 1. *Consider a set of N linear systems with state-space*

$$\dot{x}_i = A_i x_i + B_i u_i, \text{ with } A_i \in \mathbb{R}^{n\times n}, \; B_i \in \mathbb{R}^{n\times m} \text{ and } i = 1, \cdots, N$$

arbitrarily chosen from the class of controllable systems with controllability indices $\{\mu_j\}$ and $\sum_{j=1}^{m} \mu_j = n$. Let also

$$\dot{x}_{N+1} = A_{N+1} x_{N+1} + B_{N+1} u_{N+1}$$

a target linear system which belongs to the same class. Then, there are always state-feedback F_i and input G_i transformations such that

$$(sI - A_i - B_i F_i)^{-1} B_i G_i = \Phi_i (sI - A_{N+1})^{-1} B_{N+1} \tag{4}$$

with $|\Phi_i| \neq 0$ for $i = 1, \cdots, N$.

Proof. Consider a set of $N+1$ systems arbitrarily chosen from the class defined by the controllability indices μ_j. The state-space equations of the plants are given by

$$\dot{x}_i(t) = A_i x_i(t) + B_i u_i(t), \quad y_i(t) = x_i(t) \tag{5}$$

where $i = 1, \ldots, N+1$, $A_i \in \mathbb{R}^{n\times n}$, $B_i \in \mathbb{R}^{n\times m}$. The $(N+1)^{th}$ index corresponds to a target plant. There are similarity transformations P_i such that the state-space representation of all plants in the set can be reduced to canonical form with dynamics and input matrices being given as in (3). The state-space equations of the set of the N plants and the target plant in the new coordinates ($x_{ci} = P_i x_i$) are given as

$$\dot{x}_{ci} = A_{ci} x_{ci} + B_{ci} u_i, \; y_i = P_i^{-1} x_{ci} \text{ for } i = 1, \cdots, N \tag{6}$$

$$\dot{x}_{cN+1} = A_{cN+1} x_{cN+1} + B_{cN+1} u_{N+1}, \quad y_{N+1} = P_{N+1}^{-1} x_{cN+1} \tag{7}$$

respectively, with the pairs (A_{ci}, B_{ci}) for $i = \{1, \cdots, N+1\}$ having identical Brunovsky forms ($\bar{A}_c$, $\bar{B}_c$). The N plants can match the input-to-state part of the target system by applying state-feedback and input transformations

$$u_i = F_{ci,N+1} x_i + G_{i,N+1} v_i$$

with the corresponding matrices (F, G) being given as

$$F_{ci,N+1} = B_{m_i}^{-1} (A_{mN+1} - A_{m1}), \quad G_{i,N+1} = B_{m_i}^{-1} B_{mN+1} \tag{8}$$

where the state-feedback gain in the original coordinates can be recovered by $F_{i,N+1} = F_{ci,N+1}P_i$. The state-space equations of the closed-loop systems take the following form

$$\dot{x}_{ci} = (A_{ci} + B_{ci}F_{i,N+1})x_{ci} + B_{ci}G_{i,N+1}v_i, \quad y_i = P_i^{-1}x_{ci} \quad (9)$$

with $A_{ci} + B_{ci}F_{ci,N+1} = A_{cN+1}$ and $B_{ci}G_{i,N+1} = B_{cN+1}$ which are identical to the corresponding matrices of the target system. Since all the $N+1$ systems have the same dynamics and input matrices in the transformed coordinates, the state-space equations can be rewritten in the form

$$\dot{\xi} = A_{cN+1}\xi + B_{cN+1}v, \; y_i = P_i^{-1}\xi \text{ and } y_{N+1} = P_{N+1}^{-1}\xi \quad (10)$$

for $i = \{1, \cdots, N\}$. The relationship between the transfer function of the i^{th} transformed plant and the target system is given by

$$(sI - A_i - B_iF_{i,N+1})^{-1}B_iG_{i,N+1} = \Phi_i(sI - A_{N+1})^{-1}B_{N+1} \quad (11)$$

with $\Phi_i = P_i^{-1}P_{N+1}$ and $|\Phi_i| \neq 0$ since P_i and P_{N+1} are square and non-singular. This proves the theorem. □

B. Large-scale LQR problem

First the analysis of a large-scale LQR problem defined in [6] is briefly presented here. Let N_L identical systems (A,B) constitute a network described by a complete graph (i.e., the graph with all possible interconnections) which has the ability to exchange state information between any two nodes. Since the systems in the original method are considered identical the state-space form of the network shown next is obtained from augmenting the individual systems using Kronecker products:

$$\dot{\tilde{x}} = (I \otimes A)\tilde{x} + (I \otimes B)\tilde{u}, \quad \tilde{x}_0 = [x_1^T(0), \cdots, x_{N_L}^T(0)]^T \quad (12)$$

where $\tilde{x} = [x_1^T, \cdots, x_{N_L}^T]^T$ and $\tilde{u} = [u_1^T, \cdots, u_{N_L}^T]^T$. Consider now a performance index that couples the dynamical behavior of the individual systems:

$$J(\tilde{u}, \tilde{x}_0) = \int_0^\infty \sum_{i=1}^{N_L} \Big(x_i^T Q_{ii} x_i + u_i^T R u_i + \sum_{j \neq i}^{N_L} (x_i - x_j)^T Q_{ij}(x_i - x_j) \Big) d\tau \quad (13)$$

with $Q_{ii} \geq 0$, $Q_{ij} \geq 0$ and $R > 0$ or, written in a more compact form:

$$J(\tilde{u}, \tilde{x}_0) = \int_0^\infty \sum_{i=1}^{N_L} \big(\tilde{x}^T \tilde{Q} \tilde{x} + \tilde{u}^T \tilde{R} \tilde{u} \big) d\tau \quad (14)$$

where

$$\tilde{Q} = \begin{bmatrix} \tilde{Q}_{11} & \tilde{Q}_{12} & \cdots & \tilde{Q}_{1N_L} \\ \vdots & \ddots & \vdots & \vdots \\ \tilde{Q}_{N_L1} & \cdots & \cdots & \tilde{Q}_{N_LN_L} \end{bmatrix}, \quad \tilde{R} = I_{N_L} \otimes R \quad (15)$$

with $\tilde{Q}_{ii} = \sum_{k=1}^{N_L} Q_{ik}$ and $\tilde{Q}_{ij} = -Q_{ij}$.

Let $Q_{ii} = C_{ii}^T C_{ii}$ and $Q_{ij} = C_{ij}^T C_{ij}$. Under the assumption that (A,B) is controllable and all pairs (A,C_{ii}) and (A,C_{ij}) are observable, the following large scale LQR problem

$$\min_{\tilde{u}} J(\tilde{u}, \tilde{x}_0) \quad \text{s.t.} \quad \dot{\tilde{x}} = (I \otimes A)\tilde{x} + (I \otimes B)\tilde{u}, \quad \tilde{x}_0 \quad (16)$$

leads to the networked state-feedback gain $\tilde{K} = -\tilde{R}^{-1}\tilde{B}^T\tilde{P}$ where the Lyapunov function $\tilde{P}$ is the unique symmetric positive definite solution to the large scale ARE:

$$\tilde{A}^T\tilde{P} + \tilde{P}\tilde{A} - \tilde{P}\tilde{B}\tilde{R}^{-1}\tilde{B}^T\tilde{P} + \tilde{Q} = 0$$

where $\tilde{A} = I_{N_L} \otimes A$ and $\tilde{B} = I_{N_L} \otimes B$. Let now $Q_{ii} = Q_1$ and $Q_{ij} = Q_2$ with $Q_1 \geq 0$ and $Q_2 \geq 0$ then

$$\tilde{P} = \begin{bmatrix} P - (N_L - 1)\tilde{P}_2 & \tilde{P}_2 & \cdots & \tilde{P}_2 \\ \vdots & \ddots & \vdots & \vdots \\ \tilde{P}_2 & \cdots & \cdots & P - (N_L - 1)\tilde{P}_2 \end{bmatrix} \quad (17)$$

where P is the unique symmetric positive definite solution to the single-node ARE:

$$A^TP + PA - PBR^{-1}B^TP + Q_1 = 0.$$

Since $\tilde{K} = -\tilde{R}^{-1}\tilde{B}^T\tilde{P}$ the structure of $\tilde{P}$ is also preserved in the networked state-feedback gain $\tilde{K}$. For more details see [6].

C. Distributed LQR-based control for a network of non-identical linear systems

Consider N interconnected, non-identical and dynamically decoupled linear systems $(A_i, B_i), \quad i = 1, \cdots, N$ characterized by the same controllability indices $\{\mu_j\}$. The augmented state-space form of the network is given by

$$\dot{\tilde{x}} = \text{diag}(A_1, \cdots, A_N)\tilde{x} + \text{diag}(B_1, \cdots, B_N)\tilde{u}, \quad \tilde{x}(0) = \tilde{x}_0 \quad (18)$$

where $\tilde{x} = [x_1^T, \cdots, x_N^T]^T$ and $\tilde{u} = [u_1^T, \cdots, u_N^T]^T$. A stabilizing distributed control scheme is described in the following Theorem.

Theorem 2. *Consider N non-identical agents in a network with state-space form given by* (18) *and topology specified by a graph with Laplacian matrix L and maximum vertex degree d_{max}. Assume that the agents share the same controllability indices and therefore according to Theorem 1 there exist F_i, G_i and Φ_i such that* (11) *holds for all $i = 1, \cdots, N$. Consider reduced-order networked LQR problem* (16) *for $N_L = d_{max} + 1$ identical plants defined by*

$$(A_{N+1}, B_{N+1}) \triangleq (\Phi_i^{-1}(A_i + B_iF_i)\Phi_i, \Phi_i^{-1}B_iG_i)$$

and specify P and $\tilde{P}_2$ according to (17)*. Let $M = aL$ where $a > \frac{N_L}{\lambda_2(L)}$ and construct the (large-scale) state-feedback gain*

$$\hat{K} = I_N \otimes K_1 + M \otimes K_2 \quad (19)$$

where $K_1 = -R^{-1}B_{N+1}^TP$ and $K_2 = R^{-1}B_{N+1}^T\tilde{P}_2$. Let $\mathcal{N}_i$ represent the neighbourhood of the i^{th} agent. Then the state-space equation

$$\dot{x}_i = [A_i + B_i(F_i + G_iK_1\Phi_i^{-1})]x_i + aB_iG_i \sum_{j \in \mathcal{N}_i} K_2(\Phi_i^{-1}x_i - \Phi_j^{-1}x_j) \quad (20)$$

is asymptotically stable for all $i = 1, \cdots, N$.

The proof is omitted due to lack of space. Fig. 1 shows a schematic representation of the distributed scheme presented in Theorem 2 at local level i. Note that the target model may

be selected such that the perturbations in the agents models produced by state-feedback controllers are minimal in a sense that a measure of the joint model-matching control effort is minimized. This refinement of our approach is currently under investigation.

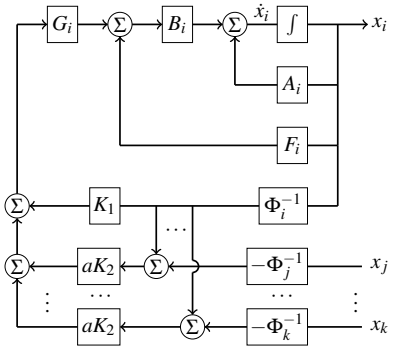

Fig. 1. Closed-loop configuration of the i^{th} agent with $(j,\cdots,k)\in\mathcal{N}_i$.

V. Simulations

In this section a formation control problem of four X-RAE1's is solved and results of numerous simulations are presented. Let four X-RAE1's move at a nominal height and exchange information about their states according to the interconnection topology shown in Fig. 2. The corresponding connected graph has maximum vertex degree $d_{max}=2$.

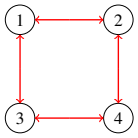

Fig. 2. Interconnection topology of the four $\{1,2,3,4\}$ X-RAE1's.

The four UAV's of the formation differ from each other with respect to their mass and symmetry about the xz plane of their body axes. Masses and products of inertia I_{xz} of each X-RAE1 are shown in Table I. The non-linear models of the four X-RAE1's are linearized for a straight flight at constant velocity $V_{T_0}=30ms^{-1}$ about the trim conditions specified in section III and the corresponding matrices of the linear systems are given in Table II. The augmented state-space form of the linearized model about the operating point of the formation is given as

$$\dot{\tilde{x}}=\text{diag}(A_1,A_2,A_3,A_4)\tilde{x}+\text{diag}(B_1,B_2,B_3,B_4)\tilde{u},\ \tilde{x}_0 \quad (21)$$

where $\tilde{x}_0=\tilde{x}(0)$, $\tilde{x}=[x_1^T,x_2^T,x_3^T,x_4^T]^T$ and $\tilde{u}=[u_1^T,u_2^T,u_3^T,u_4^T]^T$. The main control objective $\tilde{u}$ is to stabilize the formation. Further, all UAV's in the network are required to recover their vertical nominal positions in the presence of impulsive disturbances, perturbations on the trim conditions, communication failures etc. The control procedure is now presented.

Since the pairs (A_i,B_i) for $i=1,2,3,4$ have the same controllability indices, the model-matching approach proposed earlier is applied to overcome the mismatch among the linearized models. Let the linearized model (A_1,B_1) be the target system and assume that F_i, G_i and Φ_i matrices have been found such that $(A_1,B_1)=(\Phi_i^{-1}(A_i+B_iF_i)\Phi_i,\Phi_i^{-1}B_iG_i)$ for $i=2,3,4$. Consider the following LQR problem presented in IV-B with performance index $\tilde{J}$ having the same structure as in (13) for $N_L=d_{max}+1=3$:

$$\min_{\tilde{K}}\tilde{J}(v,\xi_0)\ \text{s.t.}\ \dot{\xi}=(I_3\otimes A_1)\xi+(I_3\otimes B_1)v,\ \xi(0)=\xi_0 \quad (22)$$

with weighting matrices being given as $Q_{ii}=10I_5$, $Q_{ij}=100I_5$ and $R=\text{diag}(1,100)$ for $i=1,2,3$ and $j=1,2,3$. The solution of the above LQR problem leads to the following structured lyapunov function $\tilde{P}$

$$\tilde{P}=\begin{bmatrix}\tilde{P}_1 & \tilde{P}_2 & \tilde{P}_2\\ \tilde{P}_2 & \tilde{P}_1 & \tilde{P}_2\\ \tilde{P}_2 & \tilde{P}_2 & \tilde{P}_1\end{bmatrix} \quad (23)$$

The distributed state-feedback control $\tilde{u}=\hat{K}\tilde{x}$ stabilizes (21) with

$$\begin{aligned}\hat{K}=&\text{diag}(0_{2\times5},F_2,F_3,F_4)+\\ &\text{diag}(I_2,G_2,G_3,G_4)(-I_4\otimes R^{-1}B_1^TP+\\ &M\otimes R^{-1}B_1^T\tilde{P}_2)\text{diag}(I_5,\Phi_2^{-1},\Phi_3^{-1},\Phi_4^{-1})\end{aligned} \quad (24)$$

where $P=\tilde{P}_1+2\tilde{P}_2$ and $M=aL$ reflects the structure of the graph with Laplacian matrix

$$L=\begin{bmatrix}2 & -1 & -1 & 0\\ -1 & 2 & 0 & -1\\ -1 & 0 & 2 & -1\\ 0 & -1 & -1 & 2\end{bmatrix}\quad\text{and}\quad a=1.7$$

The matrices F_i and G_i for $i=2,3,4$ can be constructed via (8) while $\Phi_i=T_i^{-1}T_1$ with T_i for $i=2,3,4$ being similarity transformations that bring the linearized models into controllable canonical form. See [11] for how to construct the T_i similarity transformations.

The nonlinear equations of motion were modelled using s-Functions in MatLab and the deviation of forward velocities and height responses from nominal values of each X-RAE1 were simulated in Simulink. The first simulation depicts height deviation and forward velocity response in the presence of non-uniform wind field which is approximated by arbitrary impulse acceleration along the vertical axis of each UAV. The distributed LQR controller (24) is applied to the non-linear model and as Fig. 3 and Fig. 4 show the height reference and the forward velocity are regulated about the nominal values.

Next, random perturbations on the initial forward and downward velocities of the four agents are considered and Fig. 5 illustrates that the distributed LQR controller stabilizes the formation and the four UAV's return to their nominal vertical positions (i.e. their heights). Note that the simulations in Fig. 3, 4 and 5 show that the formation is recovered along the vertical axis but the steady-state relative positions in the horizontal direction are altered. The longitudinal deviation along the x-axis can be regulated, if required, by additional integral action.

Finally, a simulation was reproduced under the following conditions: Agent-1 was subjected to vertical impulse acceleration representing an environmental disturbance. In addition,

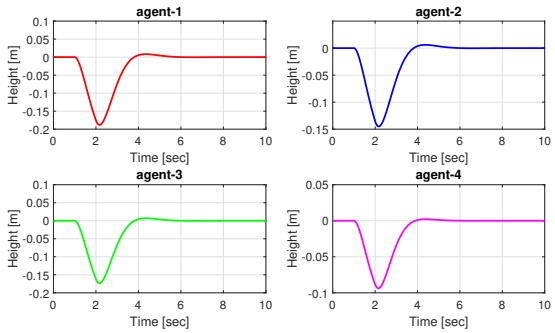

Fig. 3. Height deviation in the presence of impulse acceleration along the vertical axis.

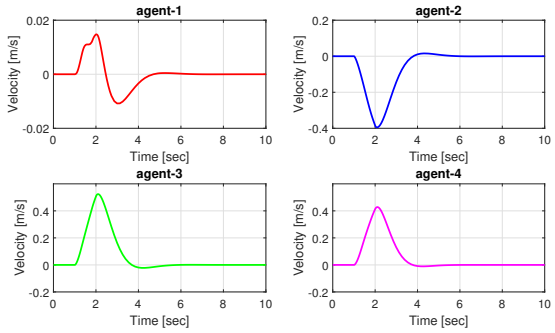

Fig. 4. Forward velocity response in the presence of impulse acceleration along the vertical axis.

agent-2 fails to transmit promptly its state to its neighbours. A Transport Delay block from the Simulink library was employed in the simulation environment to represent the delay of τ seconds over the communication channels from agent-2 to agent-1 and to agent-4. The delay was considered to be identical for both interconnections. Figure 6 demonstrates the height deviation of agent-1 and agent-2 for four different values of τ and highlights the robustness of the proposed distributed control scheme despite the presence of strong nonlinearity in the model. Further simulations were performed and robust stability was maintained for a delay up to 5 seconds.

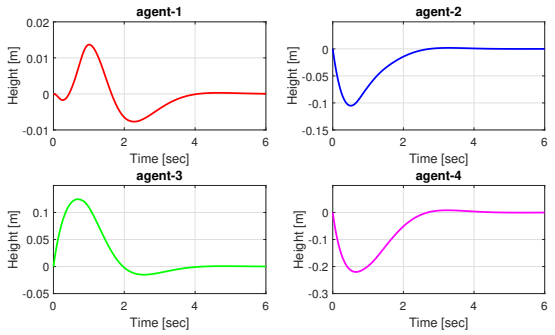

Fig. 5. Height deviation in the presence of random perturbations on the trimmed value of the downward velocity.

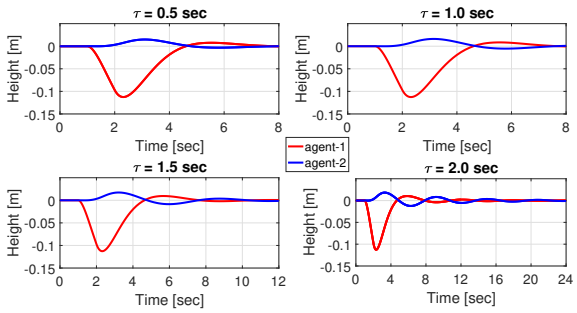

Fig. 6. Height deviation of agent-1 and agent-2 in the presence of impulse vertical acceleration in agent-1 and delay τ in the communication from agent-2 to agent-1 and to agent-4.

VI. Conclusion

We have extended an established technique for solving longitudinal stability formation control problems of UAV's to the case of non-identical dynamics. The formation flying was composed of four X-RAE1's with differences in their masses and their symmetry about the xz plane. Model-matching type techniques have been considered to map the four linearized models to a target linear system via state-feedback, input and similarity transformations. Distributed LQR control employed in networks of identical linear systems was appropriately adjusted and applied to the formation control problem. Further work is needed to extend the method to general flight conditions including lateral dynamics and therefore be implemented successfully in practical applications.

References

[1] S. Waharte, N. Trigoni, and S. J. Julier, "Coordinated search with a swarm of UAVs," in *2009 6th IEEE Annu. Commun. Soc. Conf. Sensor, Mesh Ad Hoc Commun. Networks Work. SECON Work. 2009*, 2009.

[2] J. A. Fax and R. M. Murray, "Information Flow and Cooperative Control of Vehicle Formations," *IFAC Proc. Vol.*, vol. 35, pp. 115–120, 2002.

[3] I. Tomic, E. Milonidis, and G. D. Halikias, "LQR distributed cooperative control of a formation of low-speed experimental UAVs," in *2016 UKACC Int. Conf. Control. UKACC Control 2016*, 2016.

[4] R. Kianfar, P. Falcone, and J. Fredriksson, "A distributed model predictive control approach to active steering control of string stable cooperative vehicle platoon," in *7th IFAC Symp. Adv. Automot. Control Int. Fed. Autom. Control Sept. 4-7, 2013. Tokyo, Japan*, vol. 7. IFAC, 2013, pp. 750–755.

[5] R. Olfati-Saber, "Flocking for Multi-Agent Dynamic Systems:Algorithms and Theory," *IEEE Trans. Autom. Contr.*, vol. 51, no. 3, pp. 1–20, 2006.

[6] F. Borrelli and T. Keviczky, "Distributed LQR design for identical dynamically decoupled systems," *IEEE Trans. Autom. Contr.*, vol. 53, no. 8, pp. 1901–1912, 2008.

[7] P. Deshpande, P. P. Menon, C. Edwards, and I. Postlethwaite, "Suboptimal distributed control law with H_{2} performance for identical dynamically coupled linear systems," *IET Control Theory Appl.*, vol. 6, no. 16, pp. 2509–2517, 2012.

[8] F. L. Lewis, H. Zhang, K. Hengster-Movric, and A. Das, *Cooperative Control of Multi-Agent Systems*. Springer, 2014.

[9] B. Bollobas, *Modern Graph Theory*. Springer, 2002.

[10] I. Elgayar, "Mathematical modelling, flight control system design and air flow control investigation for low speed UAVs," Ph.D. dissertation, City, University of London, 2013.

[11] P. J. Antsaklis and A. N. Michel, *Linear Systems*. New York: Birkhauser Boston, 2005.